



# Lateral Impact Response of Steel Reinforced Concrete Columns: A State-of-the-Art Review

Amna khaery khudhair<sup>a\*</sup>, Othman Hameed Zinkaah<sup>a</sup>

<sup>a</sup> Department of Civil Engineering, Al-Muthanna University, Al-Muthanna, Samawah, Iraq

\*Corresponding author E-mail: amna.k.k.civil.msc@mu.edu.iq

## Abstract

Reinforced concrete (RC) columns are critical structural elements that may experience lateral impact loading during their service life, resulting in structural responses that differ significantly from static loading conditions. This review synthesizes experimental and numerical studies on steel reinforced concrete columns subjected to lateral impact, focusing on the effects of key parameters, including impact velocity, transverse reinforcement, axial compression ratio, concrete compressive strength, longitudinal reinforcement ratio, cross-sectional dimensions, and boundary conditions. By systematically analyzing findings from previous studies, this review identifies the dominant factors governing impact resistance and clarifies their influence on dynamic response, impact force, displacement, and failure mechanisms. The results indicate that increasing impact velocity leads to higher peak impact forces, faster damage evolution, and a transition from flexural behavior to brittle shear failure. The axial compression ratio significantly affects lateral deflection, contact duration, and plateau impact force, while insufficient transverse reinforcement promotes premature shear failure. Conversely, increased stirrup reinforcement enhances confinement efficiency, delays crack propagation, and improves energy dissipation capacity. The review contributes to the current understanding of RC column behavior under lateral impact by consolidating existing knowledge and emphasizing the need for further experimental and finite element studies to support more reliable impact resistant design approaches.

**Keywords:** Concrete columns; Failure mechanisms; Impact response; Lateral impact loading; Numerical simulations; Vehicle collision

## 1. Introduction

Due to the rapid growth in reinforced concrete (RC) construction worldwide, there is an increasing need to understand the behavior of such structures when subjected to dynamic and extreme loading conditions, including impact and blast loads, as this has become a matter of significant importance [1]. Therefore, numerous studies have been performed in recent decades to interpret how concrete structures behave when experienced to extreme loads for instance explosions and impacts. Although these dynamic loads are scarce in most structures, their consequence can be disastrous and may cause structural failure [2].

Impacts, according to physicists, have short period, severe force magnitude, rapid energy dissipation, and rapid variations in object velocities [3]. It can be fall in three primary different categories according to their duration ( $t_d$ ) and severity: 1) Quasi-static loading, where the peak of the structural response occurs prior to the end of the impact period, 2) Dynamic loading, where the maximum structural response occurs at the end of impact event, and 3) Impulsive loading, where the impact time



This is an open access article under the terms of the Creative Commons Attribution License, which permits use, distribution and reproduction in any medium, provided the original work is properly cited. © 2025 The Authors

<https://www.muthuni-ojs.org/index.php/mjet/index>

ends before the structure reaches its maximal response [1]. A further classification of impact loadings can be presented according to their energy dissipating mechanism, that includes: 1) soft impact, where the initial kinetic energy was released by shocking objects, and 2) hard impact, where the impacted structure absorbed the most of the initial kinetic energy, showing minor deformation for the impactor [4].

Figure (1) illustrated the response of a structural element subjected to impact loading can be divided into two distinct stages. The initial stage is the local response, which is associated with stress wave propagation generated at the impact region and occurs within a very short time immediately after the collision. The second stage is the global response, which represents the overall behavior of the structural member, including elastic–plastic deformation and free vibration developing over a relatively longer duration throughout the entire element after impact. The overall response of the structure is mainly governed by the loading rate influence and the dynamic characteristics of the member [5].

Figure (2) illustrates the failure mechanisms that occur to a solid concrete body subjected to a collision. It includes seven missile impact effects, a) penetration, b) cone cracking, c) spalling, d) cracks with proximal and distal face, e) scabbing, f) perforation, and g) overall response [6].

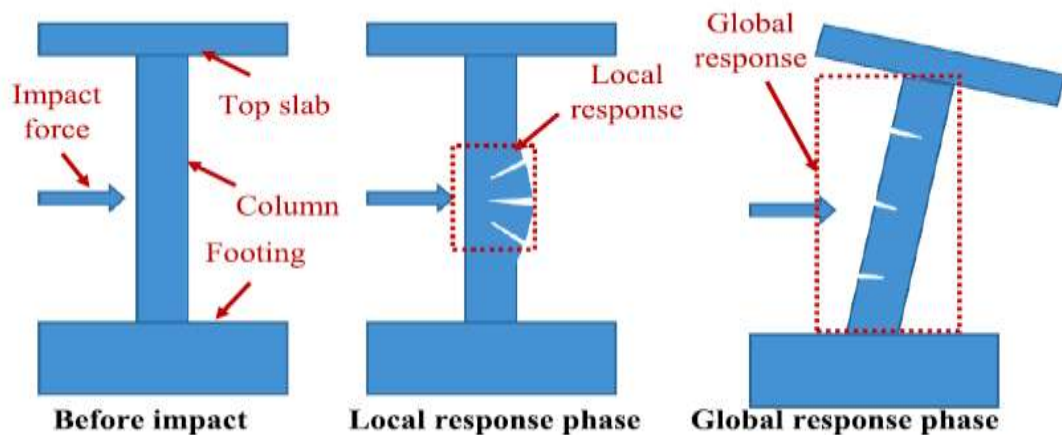


Fig. 1. Column failure under impact [7]

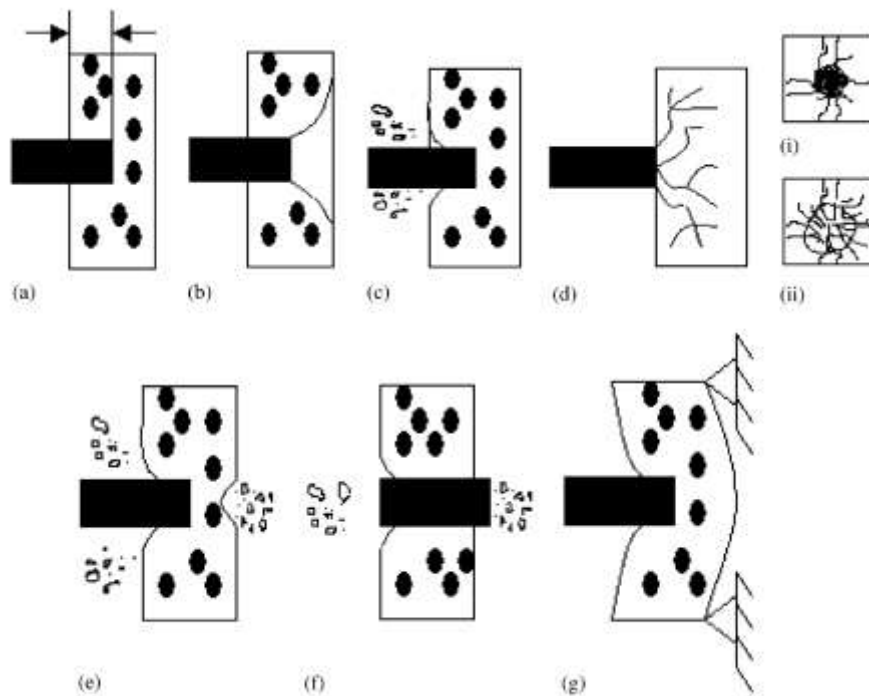


Fig. 2. Effect of impact on concrete structures [6]

In origin, columns were designed exclusively to resist gravity loads. Over time, and with the development of analytical techniques, seismic activity was incorporated into the design. Lately, the columns' susceptibility to transverse loads due to shocks has gained increasing attention [8]. Additionally, columns in buildings, bridges, electric poles and traffic signal structures, are most susceptible to vehicle impact [9], fast trains, car crashes, explosions, natural disasters, and sabotage [10]. During impact a significant shear force is transferred over a short-term interval of time, causing damage to the columns. This mechanism of resisting depends on shear, inertia, and local deformation instead of total displacement because of the short interval. Therefore, rather than static shear values, the dynamic shear capability and demand on the reinforced concrete column become significant magnitudes [9]. Although current design codes provide several simplified approaches to estimate the response of reinforced concrete (RC) structures under impact loads, they are limited in accurately representing the brittle failure mechanisms of concrete structures exposed to high-rate and impulsive loading conditions [1]. When bridge columns impacted in different location can be subjected to diverse failure patterns, i.e. flexural cracks, shear failure, punching shear failure, and brutal damage were observed in real impact events and documented as shown in Figure (3) [11].



**Fig.3.** Failure mode of bridge columns [12]

This review paper aims to use available experimental data and numerical modeling techniques to synthesize and critically evaluate the state of knowledge about reinforced concrete columns subjected to lateral impact loading. By combining knowledge from research on dynamic structural analysis, and impact behavior of reinforced concrete columns, this paper examines the key variables that influence impact force and displacement across a range of impact velocities. It seeks to clarify how these variables interact, identifying the factors that exert the strongest influence, and highlighting the parameters that require more consideration in future analysis and design.

## 2. Dynamic vs. static loading conditions

Structural members response differently under dynamic loads compared to static loads. Dynamic loads, such as impacts, required consideration of inertia effects and necessitate components with higher energy absorption capacities designed for plastic deformations to improve ductility and avoid brittle failures. Under dynamic loading, reinforced concrete (RC) elements can fail in two ways: flexural failure, which is ductile and energy-absorbing, characterized by plastic hinges and cracking, and shear failure, which is catastrophic and brittle, leading to premature failure and reduced energy absorption. Flexural failure allows the ultimate moment capacity to be reached, while shear failure results in diagonal tension cracks and failure before this capacity can be achieved [4]. Therefore, the failure mode of static loading differs than impact loading, this can be explained in a number of mechanisms. According to the inertial influence concept, the inertia response of the nearby impact zone, is the primary cause of the difference in failure mode. A further different idea, the uncoordinated effect of high strain rate on cross-section bending capacity beside resistance for shear under impact loading is what causes the failure mode to change [13]. Figure (4) shows how the internal forces distribute differently in dynamic loading from that static as a result of inertia effect ,as mentioned above This happens because dynamic analysis consider the impacts of the structure's inertia, but static analysis does not [14]. Further, for concrete, It has been demonstrated that the rate of strain has a significant impact on the experimentally measured concrete parameters, such as stiffness, fracture energy, maximum strain, strengths in compressive and tensile, such as the sample's load-carrying capacity increases as the rate of loading increases [10].

For comparison, a total of three columns were tested under horizontal static loads utilizing a contemporary horizontal impact testing system by Ye et al. [15]. The load–displacement curves derived from the impact and static tests have been compared together as shown in Figure (5) to clearly show how two curves differ from one another, the two dynamic load-displacement curves and their related static load-displacement curves are separated into three sections. It is evident from part I's curves that the impact force rose significantly due to the resistance mechanism-based inertial force generation. The maximum impact force may be several times (fluctuating from 4.51 to 15.27 times in the present study) greater than the corresponding static load value at the equivalent displacement, and the peak impact force value was developed in a very short duration.

The experimental findings presented by Huynh et al. [16], clearly show that beam-columns' structural reaction to impact loading is essentially differing from that to static loading. Impact tests showed brittle shear and flexural-shear failures, especially in axial-force-dominated high strength concrete HSC specimens, while static three-point bending tests showed flexural ductile failure in all specimens. Additionally, the dynamic energy dissipation capability exceeded static energy absorption by a large margin, sometimes by more than double. Under impact loading, it was discovered that the existence and eccentricity of axial force had a more noticeable effect, changing the impact resistance as well as the failure mode. These results demonstrate that impact performance cannot be predicted directly from static capacity.

The complexity with analysis and design of constructions subjected to dynamic sudden impact loads led to fewer studies on impact loading compared to those that examine the effects of static loads. The primary cause of this insufficient study is analysis and design complicated, which is further compounded when dealing with inelastic materials such as reinforced concrete [17].

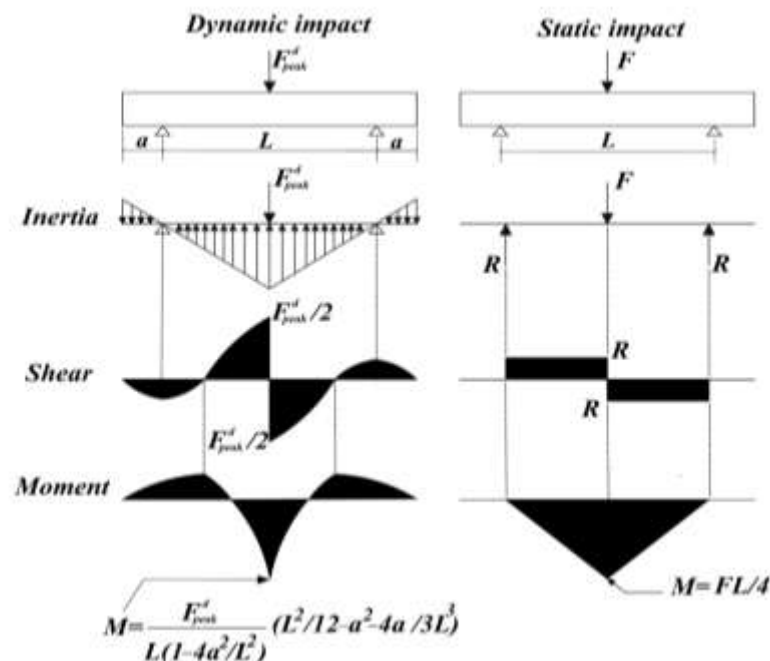
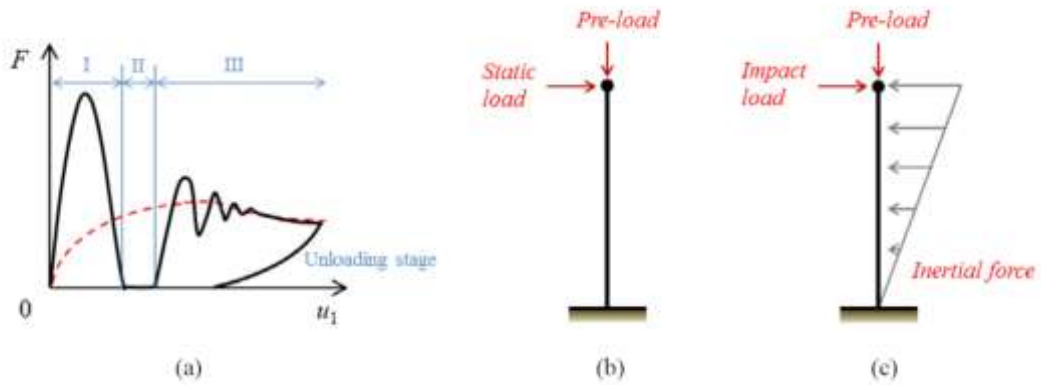


Fig. 3. Distribution of interior forces in static and dynamic analysis\ theoretical diagrams [14]



**Fig. 4.** Assessment of performance under loading of static and impact: (a) Force–displacement curve (b) Free body diagram for static loading; (c) Free body diagram for impact loading in the initial contact moment [15]

### 3. Design standards

The estimate of impact loads and the basic reactions of infrastructures exposed to various kinds of lateral impact loading are often defined by a number of design codes, particularly those resulting from collisions involving vehicles and ships using comparable static and quasi-static studies. These guidelines, however, have not taken into consideration the dynamic impacts of amplification, such as strain rate effects and inertia as follows:

- AASHTO -[18][19]: According to the FHWA Guide Specification, vessel collision loads are defined in terms of comparable static forces for structural design, which are based on experimentally verified force–deformation relationships and the kinetic energy involved in head-on vessel hits. The rules are often based on equal static impact forces obtained from extensive crash tests involving truck-barrier and tractor-trailer systems in the event of vehicle collisions. It is customary to apply a sample static force of roughly 1800 kN at a height of 1.35 m from the bottom column.
- The Japan Society of Civil Engineers (JSCE): Uses equivalent mean impact forces and energy absorption as the main design parameters in their performance-based design method for structures exposed to falling debris, such rock falls [1].
- The Australian standard AS 1170.1: Which normally takes into account masses between 1500 and 2000 kg, similarly defines vehicle impact loads in terms of equivalent static forces depending on the kinetic energy of vehicles [4].
- EN 1991-1-7-2006 [20]: Provide the Guidelines for evaluating impact and unintentional loads on buildings, with an emphasis on forces from traffic, ship impacts, and helicopter landings. For low to medium implications, it recommends employing equal static force; for severe outcomes, more sophisticated analysis is required. Because of their susceptibility to impact, parking buildings and those next to roadways or railroads are given extra consideration. To assess structural consequences, the code suggests using dynamic analysis or the equivalent static force approach, taking impact velocity and deformation behavior into account. It includes further precautions for overhead elements where clearance is less than 6m, and it specifies maximum horizontal forces of 1000 kN for truck impacts and 500 kN for automobile impacts in parking garages.
- Furthermore, the Chinese CMR (TB10002.1-2005) regulations: Use an equivalent static load formulation that is derived from the kinetic energy of the vessel to estimate ship collision actions. Through the use of a sine function, the expression specifically accounts for the impact angle, ship weight, impact velocity, and the deformation coefficients of the bridge and the vessel [21].
- According to UK Highways Agency standards: Nominal equivalent horizontal loads, usually between 250 kN and 1000 kN, should be applied to bridge piers according to experimental data [1].

### 4. Impact loading test facilities

Impact loading tests can be represented experimentally by various specially constructed testing setups as follows:

- Drop-weight impact: As seen in Figure (6), the impactor with a given mass is vertically dropped from a predetermined height in relation to the intended impact energy. It is the most popular experimental technique for examining the impact reactions of concrete components positioned horizontally, for example slabs and beams.

- Pendulum impact: As seen in Figure (7), the impactor can be launched from various angles to produce varying initial impact energy.
  - The horizontal impact : As seen in Figure (8), the impactor strikes the structure horizontally at a predetermined beginning velocity [1].
- In nature, in drop-weight loads, the dynamic performance of structural components changes slightly compared to that experiencing horizontal impact loading due to the gravitational acceleration of striking items. Consequently, the structural behavior and damage conditions may be overstated if the drop weight impact tests are used to examine the dynamic behavior of RC columns exposed to horizontal impact loads [15].

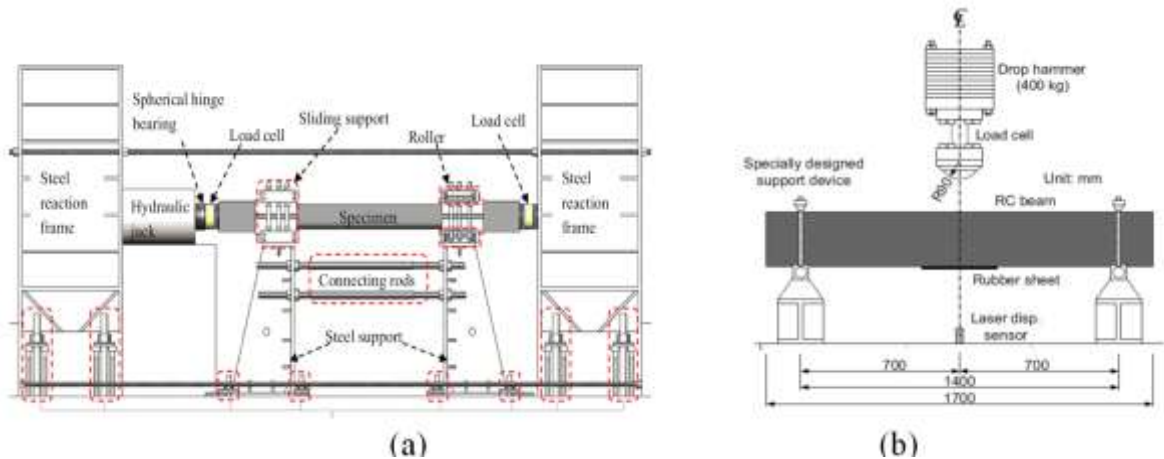


Fig. 5. Drop weight impact test.(a) [22],(b) [5]

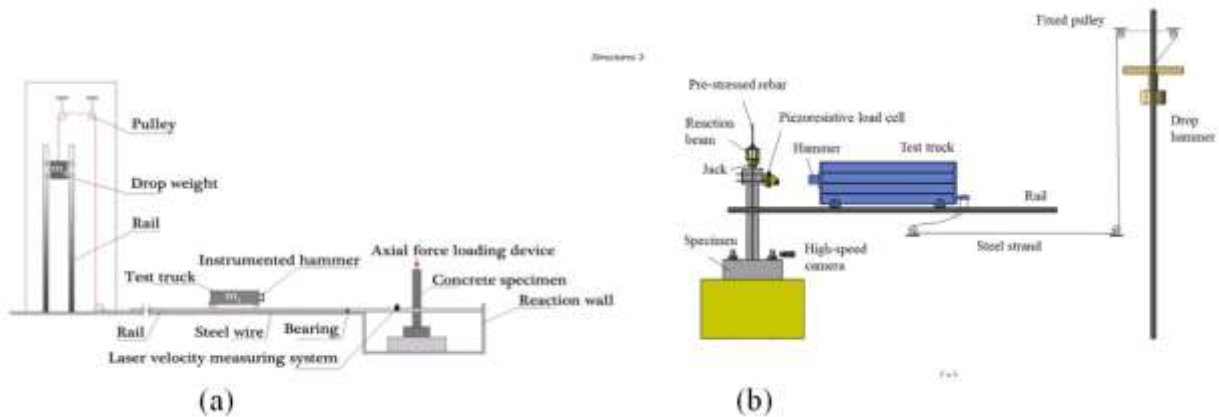


Fig. 6. Horizontal impact test (a) [23], (b) [15]

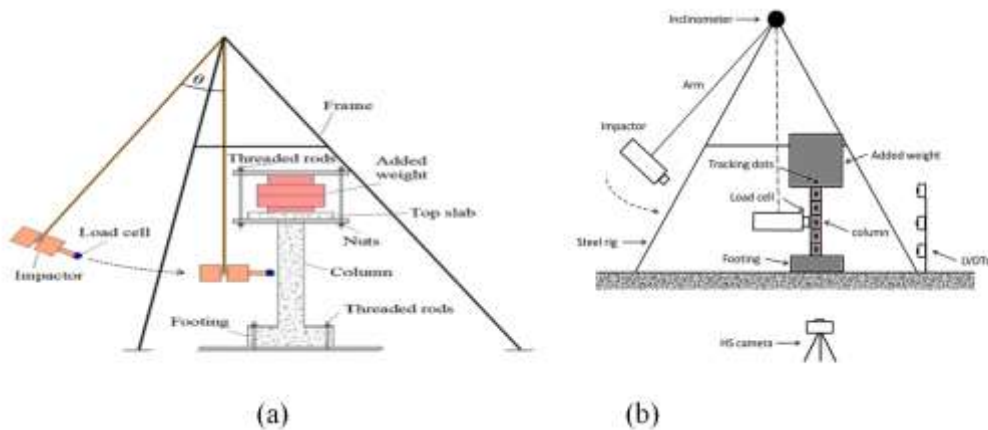


Fig. 7. Pendulum impact test (a) [24], (b) [25]

Figure (9) illustrates the frequency of testing methods for steel reinforced concrete column specimens in experimental studies that are tabulated in Table A1. It is clear to observe that test of drop weight impact is the more commonly used method, followed by horizontal impact test, while the pendulum impact test is the least utilized. This is attributed to flexibility, realistically, and simplicity of drop weight impact tests.

Furthermore, the failure mode observed in the drop-weight impact test was predominantly ductile, resulting in the formation of a plateau stage in the time history of impact force. In contrast, the horizontal impact test exhibited a brittle shear failure mode, where the maximum impact force dropped rapidly to zero without the exhibiting a plateau stage [26].

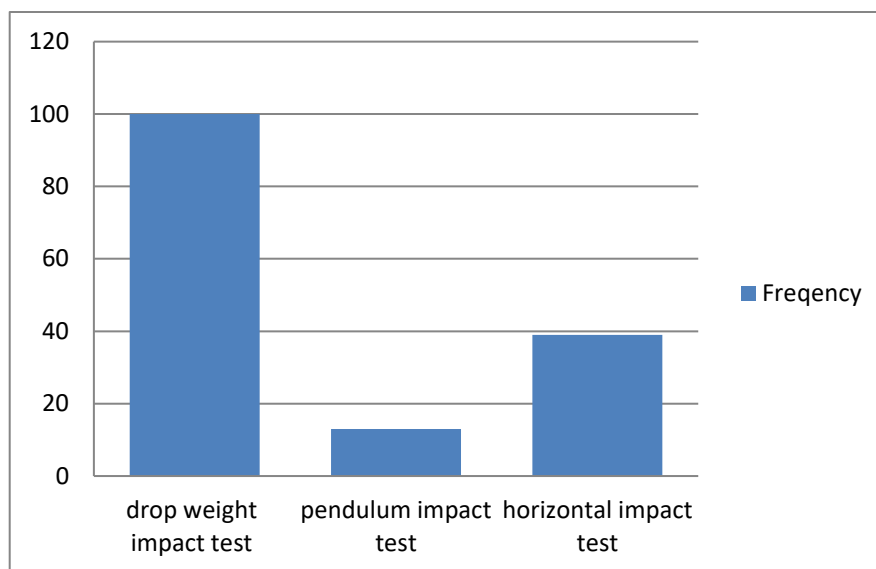


Fig. 8. Frequency of specimens tested using different impact methods

## 5. Experimental tests

Table A1 summarizes the experimental programs of previous studies conducted on reinforced concrete (RC) columns specimen experiencing to loading of lateral impact, depict cross section of specimen, longitudinal reinforcement, shear reinforcement, impact force, displacement, compressive strength and ultimate stress of steel. The main investigated parameters include stirrup spacing, impact velocity, axial load level, longitudinal reinforcement ratio, and boundary conditions as presented below:

### 5.1. Effect of shear reinforcement

The effect of shear reinforcement on the impact behavior of reinforced concrete columns has been widely investigated by numerous researchers as following : Anil et al.[17] tested in total, eight concrete column specimens with square cross-sections (three parameter was tested including insufficient stirrup, low compressive strength, and straight debar to represent old structures that not design as codes), Yilmaz et al [27] A total of 16 reinforced concrete (RC) square columns were fabricated during his experimental test. The studied variables were TRS, axial load, and energy input, A total ten of concrete column were designed by Demartino et al. [28]. In the testing process, closed hoops ( $\Phi 6$ ) with different spacing were employed to assess two types of specimens: Type 1 featured hoops measuring 100 mm, while Type 2 included hoops measuring 330 mm under cantilever and fixed-simply-supporting (volumetric transverse reinforcement ratios of 0.3% for Type 1 and 0.09% for Type 2), five specimens with circular cross-sections were performed by Zhou et al.[23],Xiang et al. [29] tested seven samples of square concrete columns, and Wang et al. [30] tested four column of all-light weight concrete.

With regard to acceleration and displacement values, the results by Anil et al. [17] and Yilmaz et al. [27] indicate that the effect of increasing the transverse reinforcement spacing (TRS) from 150 mm to 300 mm led to higher values of acceleration and displacement in the columns under impact loading. as illustrated in Figures (10) and (11) that show how the values of displacement change with TRS while keeping other parameters constant. The details of collected specimens from Anil and Yilmaz tests are illustrated in Table A1, same result found by Demartino et al. [28] when increase spacing from 100 to 330 under same impact velocity and same boundary conditions, Xiang et al. [29] with increasing spacing from 100 to 200 mm displacement increase, and with Wang.et.al.[30] when increasing stirrups ratio from 0.27 % to 0.4 %. On the other hand, there is no obvious change in the midspan displacement peak value when the stirrup reinforcement ratio increases was noticed by Zhou et al.[23] as shown in Figure (12) that explain how the values of TRS can effect on impact response and displacement value, the details of specimens from Zhou test were illustrated in Table A1.

In terms of impact force, A comparison by Demartino et al. [28] of the high-velocity tests reveals that the impact force in specimen with spacing 330 mm declines more steeply than in those with spacing 100 mm. This reduction indicates that the column with insufficient shear reinforcement endured more significant damage and greater reduction in stiffness. an increase in the stirrups spacing leads to an increase in both maximum force and impact time at similar impact speed and axial ratio, but the plateau force is almost the same in all cases of spacing change was noticed by Xiang et al. [29]. Moreover, Wang.et.al. [30] found that as stirrup ratio increase, the impact force increases as well as, overall stiffness of the column. The opposite for the findings by Zhou et al.[23] which indicated that the initial contact stiffness and maximum impact force do not considerably change as stirrup spacing increases, as well as the platform stage's duration.

With regard to mode of failure, all the above studies found that the backing provided by increasing the spacing enhances column integrity and reduces crack development and propagation. Moreover, Stirrup ratio can efficiently manage the failure mode from flexure to shear and there was an expansion in both the number and width of shear cracks in the columns when the TRS increased.

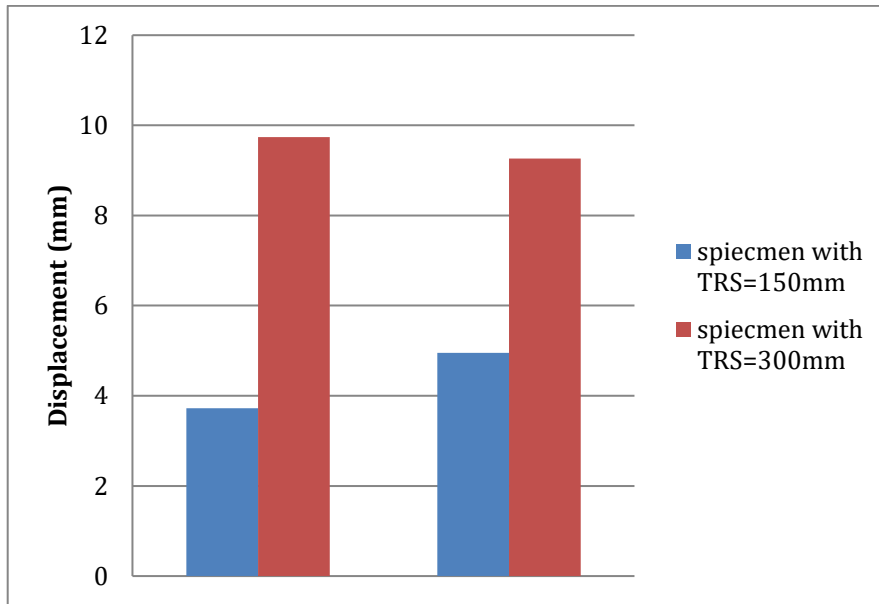


Fig. 9. Effect of TRS on values of displacement.

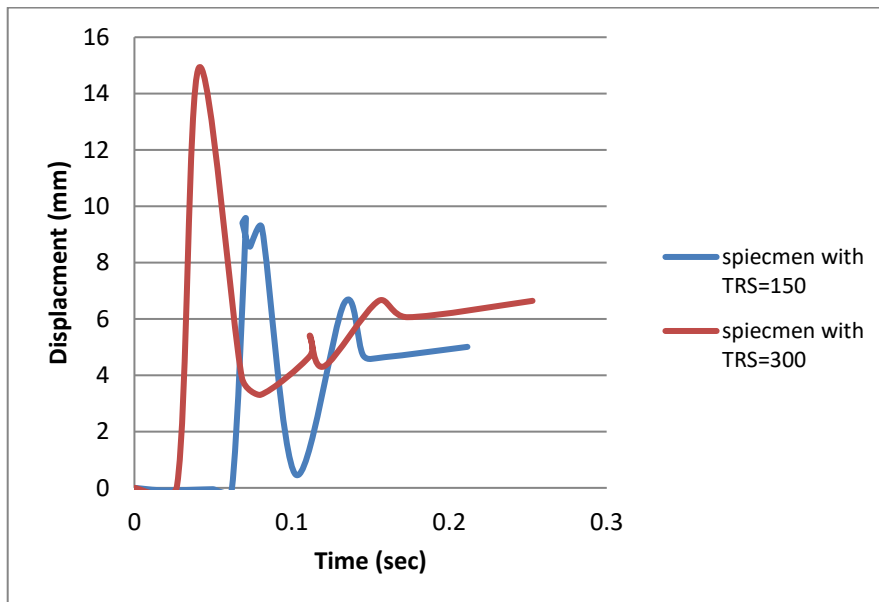
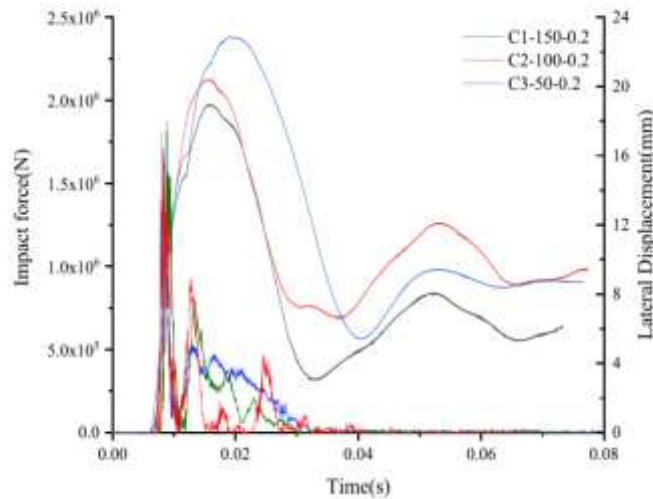


Fig. 10. Effect of TRS on values of displacement



**Fig. 11.** Effect of stirrup spacing on the impact force and lateral displacement histories of the specimens [23]. The left vertical axis represents the impact force, while the right vertical axis represents the lateral displacement

## 5.2. Effect of impact velocity

One of the most important factors influencing the dynamic response and failure mechanism of reinforced concrete columns exposed to lateral impact loads is impact velocity. In order to measuring the effect of different impact velocities, numerous experimental investigations have been conducted as following: Two cases of input impact energy ( $E=0.5 \text{ mv}^2$ ) were investigated by Yilmaz et al.[27]; one case with input impact energy of  $0.824 \text{ kN}\cdot\text{mm}$  (velocity =  $4.43 \text{ m/s}$ ) and other with value of  $1.236 \text{ kN}\cdot\text{mm}$  (velocity= $5.42 \text{ m/s}$ ), Using pendulum test setup, six reinforced concrete columns were conducted under varying axial compression ratios and impact speeds (low velocity= $2.85 \text{ m/s}$ , medium velocity =  $3.58 \text{ m/s}$ , and high velocity =  $4.85 \text{ m/s}$ ) by Sun et al. [31], Demartino et al. [28], Liu et.al. fabricated ten circular reinforced concrete column specimens in total [22], Chen et al. [32] to mimic the scenario of a heavy vehicle colliding with a reinforced concrete column, Xiang et al. [29], and Li et.al. [26] tested six piers specimens by using horizontal impact system with two key factors impact velocity and longitudinal reinforcement.

Regarding to displacement, the results by Yilmaz et al. [27] Sun et al. [31], Chen et al. [32], Xiang et al [29], and Li et.al. [26], are indicated that an increase in impact speed produces more intense force pulse, resulting in greater localized damage at the point of impact and increased deflection in the mid-span as seen in Figure (13) that shows a comparison of values of displacement for specimens by Sun et al. [31], the details of specimens are illustrated in Table A1. While Demartino et al. [28] noticed that at low impact velocity, minor damage was observed, while at medium and high impact velocities, a large reduction in stiffness and higher lateral displacements occurred. In regard to impact force, Yilmaz et al.[27] observed that the increase in the input impact energy led to increase in impact load, as observed in Figure (14) which illustrates the effect of impact velocity (input energy) on the peak impact force under different axial load levels (0, 20, 40, and 60 kN). The notation (0/0.824) represents zero axial load with an input energy of  $0.824 \text{ kN}\cdot\text{mm}$ , whereas (20/1.236), for instance, indicates an axial load of 20 kN with an input energy of  $1.236 \text{ kN}\cdot\text{mm}$  parallel to the higher velocity situation, the details of specimens are illustrated in Table A1. Sun et al. [31] noted that as the impact velocity and the axial compression rate increase both the maximum impact force and the duration of the impact on the force platform rise. Demartino et al. [28] indicated that the higher initial kinetic energy caused the column's inertial resistance to increase during the contact phase, the peak impact force increased nearly proportionately to the impact velocity. Xiang et al [29] noted that increasing the impact height considerably intensified the damage sustained by the tested samples, a higher drop height resulted in greater peak impact force, higher plateau force, and a longer impact period. In terms of failure mode, the findings from studies above found that increasing the impact of velocity leads to higher impact energy and more severe damage in columns. at higher velocities, the damage concentrated around the impact area, resulting in diagonal shear cracks and concrete crushing. Consequently, as the velocity elevates, the column becomes more susceptible to shear failure. It is important to note that samples exposed to low speeds exhibit a failure pattern similar to static load failure or bending failure [15].

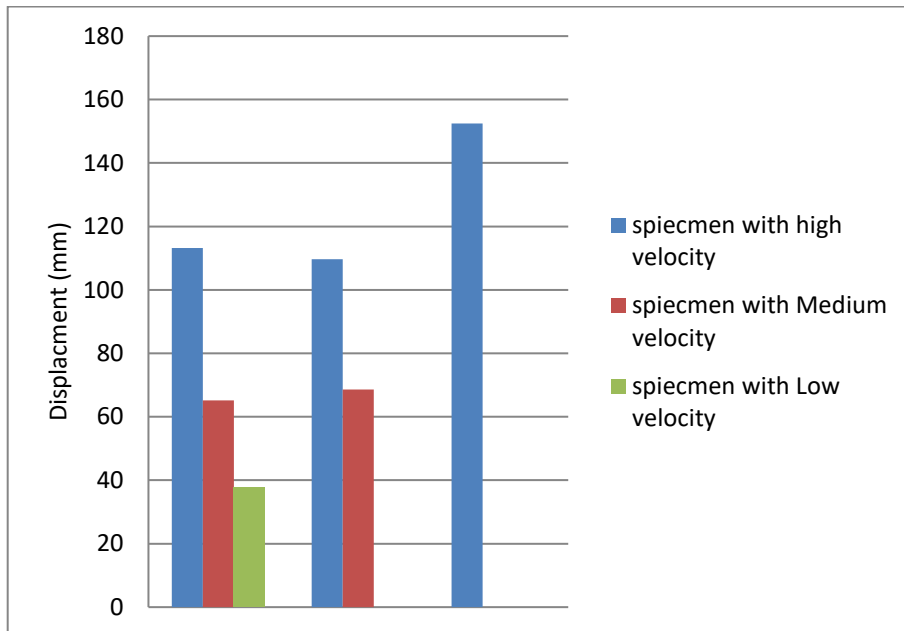


Fig. 12. Influence of impact speed on displacement

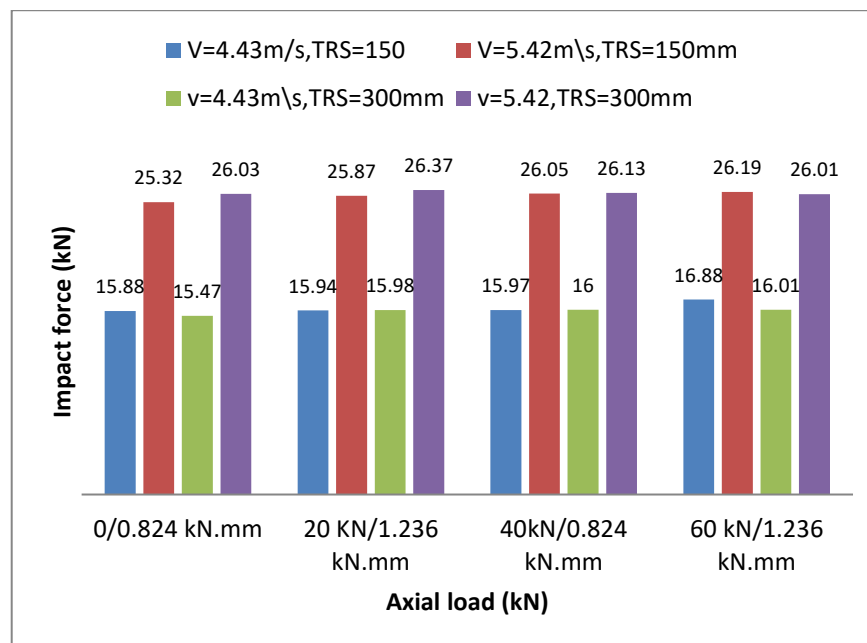


Fig. 13. Effect of input impact energy on impact force

### 5.3. Effect of axial load

Based on previous tests, under impact loading, it is observed that the axial loads have an significant effect on the columns' dynamic responses [22]. Various studies investigate steel reinforced column under impact loading with different axial load ratios as following: Yilmaz et al. [27], Sun et al.[31] , Ye et al. [15], Liu et al. [22] ,Luo et al. [13], Xiang et al. [29] .

In terms of displacement and acceleration, Yilmaz et al.[27] demonstrates that under the assumption that the input impact energy and transverse reinforcement spacing stay constant, the peak acceleration values measured increase and RC columns' peak and residual mid-point displacement magnitude decrease with the applied axial load. The residual displacements are permanent deformation recorded after the end of vibrations caused by impact load. However, it has been shown that columns which are axially loaded near the value of balanced axial load have suffered significant damage, and their residual displacements have grown dramatically. This is because increasing the imposed axial load toward the balanced limit magnitude decreases the ductile behavior and increases the second-order bending moment (termed as the P- $\Delta$  effect). Besides, energy dissipation ability reduced with the increase of axial loads for specimens with same input impact energy and

shear reinforcement, as shown in Figure (15) which illustrates the effect of axial load (0, 20, 40, and 60 kN) on the energy dissipation capacity under different input energy levels. The notation (0/0.824) represents zero axial load with an input energy of 0.824 kN·mm, whereas (20/1.236), for instance, indicates an axial load of 20 kN with an input energy of 1.236 kN·mm, the details of specimens are illustrated in Table A1.

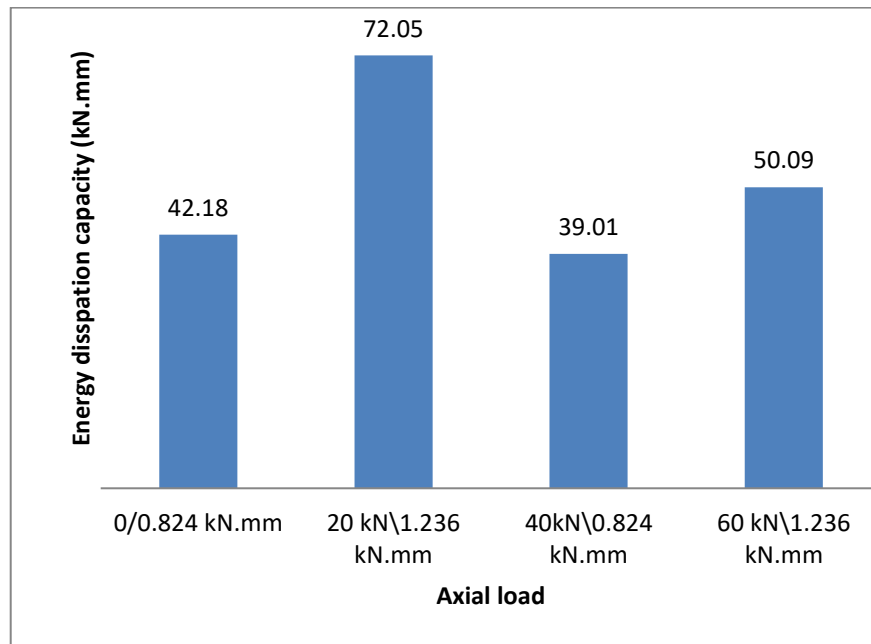
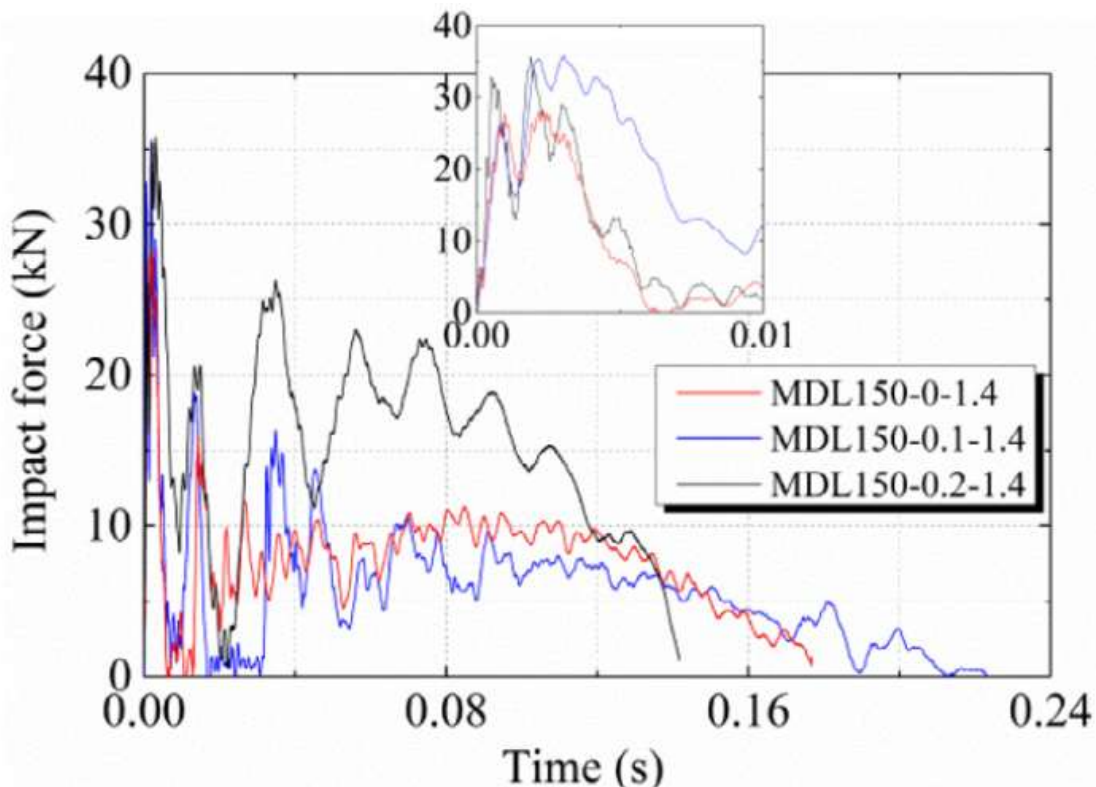


Fig. 14. Relation between axial load and energy dissipation

Same finding was found by Sun et al [31] was noted that the amount of displacement reduces initially with rising the axial ratio, and at a certain level an opposite response occurs. Comparable findings were found by Ye et al. [15] The residual deformation of the column following impact was influenced by the presence of axial compressive load. The columns with axial pre-load nearly always returned to its primary situation throughout the rebounding process, indicating that reinforced concrete columns exposed to impact loads benefit from the presence of axial pre-load in terms of deformation restoration. With respect to impact force, the observed findings showed that as the axial compressive ratio increases, a little effect will occur to specimens with keeping other parameters constant as shown in Figure (16), details of specimens illustrated in Table A1.



**Fig. 15.** Effect of axial compressive ratio on impact force [15]

Liu et al. [22] demonstrate that the existence of axial force may cause (P- $\Delta$ ) effect, especially for high impact energy. In terms of impact force, the column with axial load has maximum impact force higher than column with no axial force, this due to axial load enhance contact stiffness. The application of axial load caused a reduction in vertical displacements at small deformation levels. Luo & Wang [13]. Found that under an axial compression ratio of 0.2, the stiffness of the column was temporarily enhanced, affecting the development of cracks and deformation mode. And The outcomes from Zhou et al [23] showed that there was a significant effect on flexural rigidity when an increase in axial ratio happened. Moreover, peak impact force rises by 10% at the equal impact velocity as the axial compression ratio increases. In the same way, the mid-span displacement effected by the beneficial influence of the large axial compression ratio, the substantial axial compression effectively prevents the mid-span displacement from developing during the column collision process. Similar results by Xiang et al [29] that indicated that the axial compression ratio enhance column stiffness and reduce lateral deflection within a certain range; however, according to the P- $\Delta$  effect, excessive axial load combined with large lateral displacement may amplify instability.

#### 5.4. Effect of reinforcement ratio

In terms of displacement, the results by Ye et al. [15], Li et.al. [26], and Wang.et.al. [30], revealed that maximum displacement and residual displacement were both decreased for specimens with higher longitudinal ratio. In terms of impact force, the outcomes of Ye et al. [15] clarified that the average impact force ( $F_{ave}$ ) was significantly enhanced by the ratio of longitudinal reinforcement ( $\rho$ ). As  $\rho$  increased from 1.4% to 2.7%,  $F_{ave}$  rose from 5.92 kN to 11.13 kN, marking an 88% increase. comparable results were found by Wang.et.al. [30], increasing the longitudinal reinforcement ratio enhances the column's initial stiffness, which in turn raised the peak impact force. In contrast with findings by Li et.al. [26] that indicated under different ratios, the maximum impact force remained largely unaffected. because the influence of longitudinal ratio on local stiffness of column is not substantial. Liu et al. [22] critically, find that axial loads can lead to severe consequences for columns with a lower reinforcement ratio when they experience a high-energy impact. Increasing the reinforcement ratio significantly reduces both overall and local failures of column samples. Li et.al. [26] found that the severity of damage and cracks width decrease with rising longitudinal reinforcement ratio. Figure (17) shows that increasing the longitudinal reinforcement ratio led to enhance the residual stiffness and reduce the dissipation of energy.

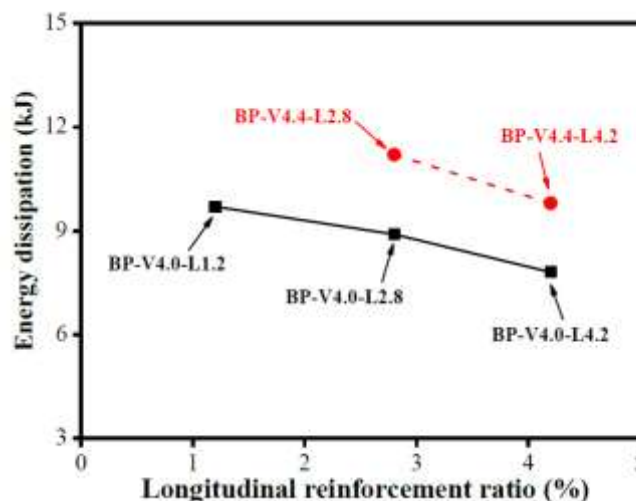


**Fig. 17.** Effect of longitudinal ratio on energy dissipation [26]

#### 5.5. Effect of Concrete compressive strength

Anil et al. [17] studied the effect of compressive strength on the impact response of concrete columns. In terms of acceleration, it is found that columns with low concrete strength (10 MPa) exhibited lower acceleration measurements due to their reduced stiffness and associated energy loss ability. In contrast, columns made of higher strength concrete have a greater accelerations magnitude because of their higher stiffness and toughness with equal energy. The same with displacement. With respect to impact loads, the results indicate that structural elements with higher strength concrete have a greater impact loads and energy

ability than those made from reduced compressive strength. When combining the impact load- time curves for two specimens (Presented in Table A1) with the same (TRS) but different compressive strength as shown in Figure (18), it can be noting how impact load effected by the increase in compressive strength. Furthermore, there were minor fluctuations in TRS effect observed in specimens with higher-strength concrete (20 MPa), suggesting that stronger concrete mitigates the effect of TRS on the dynamic behavior to impacts.

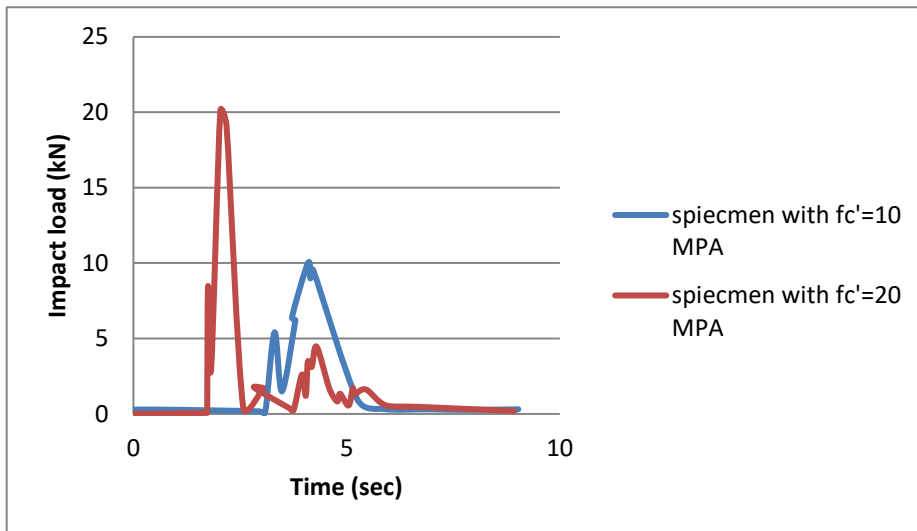


**Fig. 18.** Effect of compressive strength on impact load

In addition, Wei et al. [33] studied the improvement of concrete strength when changing from traditional reinforced concrete (RC) to ultra-high-performance concrete (UHPC) using square and circular cross sections test specimens, each of which included both RC and UHPC columns. According to experimental results, when exposed to the impact scenario, square and circular UHPC columns displayed relatively little flexural damage, while both square and circular columns showed brittle shear failures along with significant concrete splitting.

### 5.6. Effect of Boundary Conditions

The cantilever case (C case) and the fixed case (F case) were the two boundary condition scenarios that were investigated by Demartino et al. [28]. Boundary circumstances were shown to have a negligible impact on the maximum impact force. Figure (19), which illustrates how boundary circumstances affect the impact force for samples with a similar transverse reinforcement spacing (TRS) and impact velocity, generally demonstrates that the impact force reported in the C case was marginally lower than that in the F case. Consequently, the specimen with the F test was exposed to more damage than the other tests, which resulted in a greater impact force and linked impulse value. Regarding displacement, the F test showed a higher maximum displacement value than the C test, even though the impact velocity was the same.

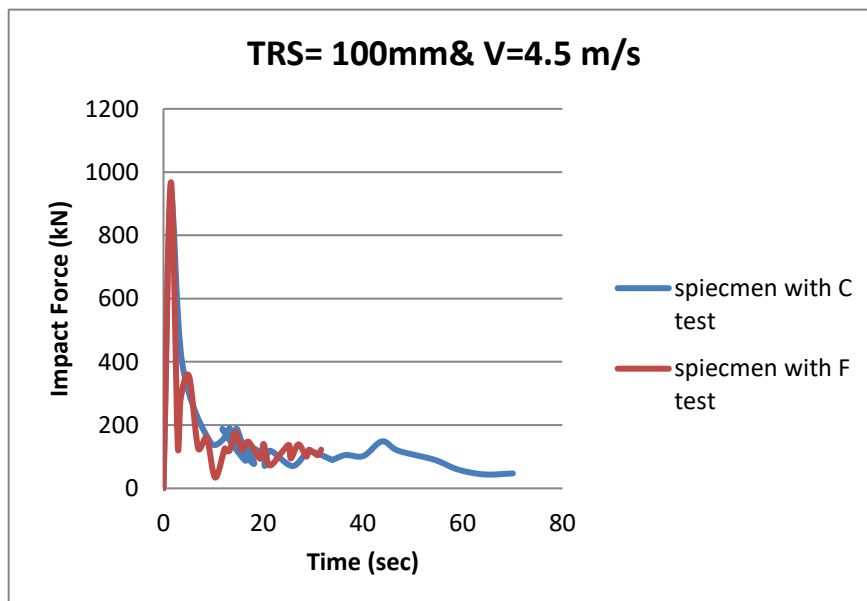


**Fig. 19.** Effect of boundary conditions on impact force

### 5.7. Effect of section width

Ye et al. [15] observed that flexural stiffness significantly influences the duration of the impact but has minimal effect on the peak impact force. This is due to the fact that at the moment of initial impact, the horizontal impact force is primarily countered by inertial force rather than by global structural bending deformation. Consequently, the ratio of peak impact force to static force ( $F_p/F_{su}$ ) prone to increase as the width ( $w$ ) decreases. For displacement, as presented in Figure (20) that comparing specimens with different width cross section while keeping other parameters constant, specimens with a greater  $w$  value exhibited lower maximum displacement ( $u_{max}$ ) and residual displacement ( $u_{res}$ ) upon completion of impact testing, the details of specimens illustrated in Table A1.

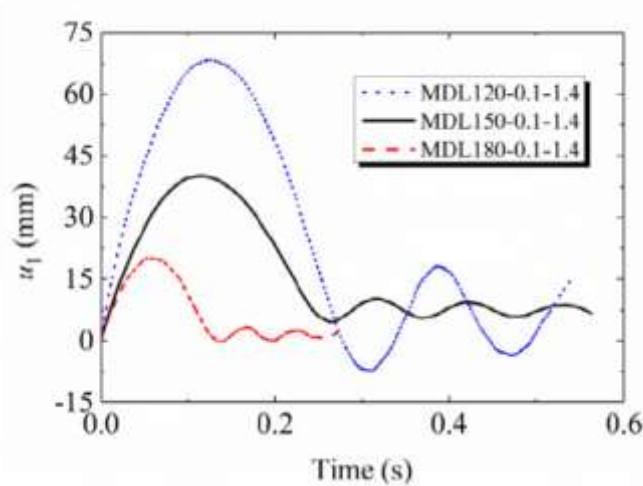


Fig. 16. Effect of section width on displacement[15]

### 5.8. Effect of load application point

Another variable investigated by Anil et al. [17] was the impact location. The damage distribution was more uniform and concentrated near the top and bottom supports, when the impact load was imposed along the axis of symmetry of the column. In this case, fewer shear cracks were observed, and those that developed were relatively narrow. In contrast, when the impact load was applied eccentrically (i.e., away from the axis of symmetry), both the number and width of shear cracks increased significantly, particularly close to one end of the column. It is noteworthy that specimens with less transverse reinforcement spacing (TRS) and those subjected to impact near the column end experienced more severe damage, as illustrated in Figure (21), the details of the specimens are illustrated in Table A1.



Fig. 17. Crack distribution of the samples [17]

## 6. Finite element studies

Experimental studies investigating the impact behavior of RC beams have provided important observations and useful experimental data. However, conducting such tests is costly and requires considerable time and resources. Moreover, several response parameters are difficult to capture experimentally, including the concrete stress distribution near the impact region, internal shear forces, and bending moments. Consequently, finite element modeling has been widely adopted to obtain more detailed insights and to perform comprehensive parametric investigations. Nevertheless, developing reliable numerical impact models requires careful consideration of several aspects, such as contact interaction techniques, constitutive material formulations, failure and damage criteria, dynamic increase factors (DIF), and erosion approaches. These numerical techniques and modeling considerations are discussed in this section [34]. Most studies are conducted using either LS-DYNA software or ABAQUS for dynamic analysis. A summary of selected relevant studies provided in the following section.

Three-dimensional finite element analysis is considered an effective approach for accurately simulating the nonlinear behavior of reinforced concrete structures under impact loading. Unlike simplified beam or two-dimensional models, 3D FE models can better capture complex phenomena such as concrete cracking, crushing, confinement effects, and stress redistribution under multiaxial stress conditions. Therefore, advanced numerical modeling serves an important function in predicting the impact response and failure mechanisms of reinforced concrete columns. The implementation of concrete constitutive laws in finite element analysis remains challenging due to the heterogeneous and discontinuous nature of concrete. In particular, crack propagation is commonly simulated using either discrete crack or smeared crack approaches. Although the discrete crack approach can represent physical cracking more realistically, it often requires predefined crack paths or remeshing techniques. On the other hand, the smeared crack approach is more compatible with FE formulations but may overestimate the shear resistance of structural members. In addition, steel reinforcement can be modeled using discrete, embedded, or smeared reinforcement techniques, with previous studies indicating that the selected reinforcement modeling approach has limited influence on the overall numerical results [35]

Columns made of different materials were analyzed under lateral impact using the LS-DYNA software by Yu et al. [36]. The results showed that the vehicle's mass and stiffness have a clear effect on the value of the impact force, and that the impact force increases with increasing speed, but in a non-linear relationship. Regarding the boundary conditions, their effect was minimal as mentioned in experimental analysis by Demartino et al. [28] which discussed in previous section, while the type of material of column had a substantial influence on the impact force, especially at high impact speeds.

In order to mimic experimental testing on concrete and reinforcing steel, a nonlinear finite element model was generated in LS-DYNA by Sha et al. [37]. The results, which included impact force, time, displacement, and damage, were in agreement with the experimental data. After validation, parametric investigations on a number of parameters were made easier by a full-scale barge-pier collision model. Important results showed that while barge tonnage influences duration and impulse, impact velocity significantly influences peak force. While pier height and superstructure mass have little effect on peak force but change structural reaction, pier diameter has a limited effect on peak force but greatly affects displacement response. Furthermore, the soil–foundation interaction has a negligible impact on peak force but influences post-impact vibrations and displacement, and the impact location does not significantly alter peak force but increases displacement at higher heights.

Detailed numerical models were developed by Zhou et al. [38] to simulate a vehicle collision with a pier, and the resulted damage was analyzed. The results showed that the failure process is separated into four-time phases: an initial peak, then force development, followed by a maximum peak, and finally force decline. At the maximum peak, shear failure occurs with spalling of the concrete and fracture of the stirrups where both impact force and displacement reach their maximum value simultaneously.

Table A2 summarizes additional numerical studies, with particular focus on research involving parametric investigations. Moreover, most of the numerical studies presented in the table showed good agreement with experimental results, demonstrating the effectiveness and reliability of finite element models in simulating the impact behavior of reinforced concrete members.

## 7. Conclusion

This paper provides a state-of-the-art review of structural responses and failure behaviors of reinforced concrete columns subjected to lateral impact loads. Firstly, the difference between static and dynamic loading conditions, as well as the most commonly used design codes and impact facilities were introduced. Then, the most parameters that affect impact force, displacement, and failure mode were discussed. The available finite element studies were presented and summarized in tabulate form. The review study shows that:

1. Impact loading on reinforced concrete columns poses a significant hazard to structural safety and human life. Unlike static loading, dynamic impact loading produces different responses in terms of failure mode, impact force, and lateral displacement. Therefore, the behavior of reinforced concrete columns under impact loading requires further

investigation to improve impact resistant design.

2. Most previous studies indicated that impact velocity is the governing determinant controlling the failure mode of reinforced concrete columns. Flexural failure was commonly observed under low impact velocities, flexural–shear failure under moderate velocities, and brittle shear failure under high impact velocities. In addition, the impact force was found to increase approximately linearly with increasing impact velocity, particularly at high velocity levels.
3. Preceding literature reported varying conclusions regarding the influence of axial force on impact behavior. However, most findings suggested that a moderate axial compression ratio can improve the impact resistance and overall structural performance of reinforced concrete columns under lateral impact loading by increasing stiffness, moment capacity, and overall strength while reducing maximum and residual displacements. However, when the axial load ratio overcomes a critical threshold (approaching the balanced condition), this beneficial effect diminishes, and residual displacement increases due to second-order ( $P-\Delta$ ) effects, potentially reducing overall impact resistance.
4. Limited studies have investigated the influence of shear reinforcement ratio, concrete compressive strength, longitudinal reinforcement ratio, boundary conditions, and column cross-section on the impact behavior of reinforced concrete columns.
5. Generally, to prevent brittle failure, the design should include higher compressive strength, a sufficient stirrups ratio, and the application of load close to middle of the column. As well as, the increase in concrete strength led to increase in acceleration, displacement, and impact loads this led to enhancing the overall impact performance of the columns. Furthermore, higher compressive strength reduces the sensitivity of column behavior to transverse reinforcement spacing. And the increase in the longitudinal reinforcement ratio resulted in increase of impact force and improved energy dissipations.
6. Numerical simulation performed using LS-DYNA or ABAQUS software has been shown accurately representing the dynamic response of the impacted columns, represented cost effective tools compared to laboratory tests.

Finally, there is a need for more studies, whether experimental, numerical or theoretical, to better predict the Columns response under lateral impact, such as : columns in building subjected to higher axial loads, full-scale columns, develop a reliable design procedure for impact-resistant RC columns, and formulate efficient FE models that are less sensitive to parameter variation, thereby ensuring safety under sudden conditions.

## Reference

- [1] C. Zhang, G. Gholipour, and A. A. Mousavi, *State-of-the-Art Review on Responses of RC Structures Subjected to Lateral Impact Loads*, vol. 28, no. 4. Springer Netherlands, 2021. doi: 10.1007/s11831-020-09467-5.
- [2] A. M. Remennikov and S. Kaewunruen, “Impact resistance of reinforced concrete columns: Experimental studies and design considerations,” *Prog. Mech. Struct. Mater. - Proc. 19th Australas. Conf. Mech. Struct. Mater. ACMSM19*, pp. 817–823, 2007.
- [3] L. Yanhui *et al.*, “Numerical study on existing RC circular section members under unequal impact collision,” *Sci. Rep.*, vol. 12, no. 1, p. 14793, 2022, doi: 10.1038/s41598-022-19144-1.
- [4] H. M. I. Thilakarathna, “Vulnerability Assessment of Reinforced Concrete Columns Subjected to Vehicular Impacts,” no. December, 2010.
- [5] K. Fujikake, B. Li, and S. Soeun, “Impact Response of Reinforced Concrete Beam and Its Analytical Evaluation,” *J. Struct. Eng.*, vol. 135, no. 8, pp. 938–950, 2009, doi: 10.1061/(asce)st.1943-541x.0000039.
- [6] Q. M. Li, S. R. Reid, H. M. Wen, and A. R. Telford, “Local impact effects of hard missiles on concrete targets,” *Int. J. Impact Eng.*, vol. 32, no. 1–4, pp. 224–284, 2005, doi: 10.1016/j.ijimpeng.2005.04.005.
- [7] T. M. Pham, W. Chen, M. Elchalakani, T. V. Do, and H. Hao, “Sensitivity of lateral impact response of RC columns reinforced with GFRP bars and stirrups to concrete strength and reinforcement ratio,” *Eng. Struct.*, vol. 242, no. April 2021, p. 112512, 2021, doi: 10.1016/j.engstruct.2021.112512.
- [8] M. Abedini, A. A. Mutalib, J. Mehrmashhadi, S. N. Raman, R. Alipour, and T. Momeni, “Large Deflection Behavior Effect in Reinforced Concrete Columns Exposed to Extreme Dynamic Loads”.
- [9] H. Sharma, S. Hurlbaas, and P. Gardoni, “Performance-based response evaluation of reinforced concrete columns subject to vehicle impact,” *Int. J. Impact Eng.*, vol. 43, pp. 52–62, 2012, doi: 10.1016/j.ijimpeng.2011.11.007.
- [10] E. Energy, “Performance of FRP-Strengthened Reinforced Concrete Columns under Impact Loading Alaa Omar Moftah Swesi,” no. October, 2021.
- [11] T. V. Do, T. M. Pham, and H. Hao, “Dynamic responses and failure modes of bridge columns under vehicle collision,” *Eng. Struct.*, vol. 156, no. November 2017, pp. 243–259, 2018, doi: 10.1016/j.engstruct.2017.11.053.
- [12] T. V. Do, T. M. Pham, and H. Hao, “Proposed design procedure for reinforced concrete bridge columns subjected to vehicle collisions ( a ) The schematic view of the prototype bridge specimen,” vol. 22, no. March, pp. 213–229, 2019.
- [13] Z. Luo and Y. Wang, “Experimental and numerical study of axially loaded reinforced concrete columns and frame columns under lateral impact loading,” *Can. J. Civ. Eng.*, vol. 49, no. 3, pp. 330–345, 2022, doi: 10.1139/cjce-

2020-0590.

- [14] G. Gholipour, C. Zhang, and A. A. Mousavi, "Effects of axial load on nonlinear response of RC columns subjected to lateral impact load: Ship-pier collision," *Eng. Fail. Anal.*, vol. 91, no. November 2017, pp. 397–418, 2018, doi: 10.1016/j.engfailanal.2018.04.055.
- [15] J. Bin Ye, J. Cai, Q. J. Chen, X. Liu, X. L. Tang, and Z. L. Zuo, "Experimental investigation of slender RC columns under horizontal static and impact loads," *Structures*, vol. 24, no. July 2019, pp. 499–513, 2020, doi: 10.1016/j.istruc.2020.01.034.
- [16] L. Huynh, S. Foster, H. Valipour, and R. Randall, "High strength and reactive powder concrete columns subjected to impact : Experimental investigation," *Constr. Build. Mater.*, vol. 78, pp. 153–171, 2015, doi: 10.1016/j.conbuildmat.2015.01.026.
- [17] O. Anil, M. Cem Yilmaz, and W. Barmaki, "Experimental and numerical study of RC columns under lateral low-velocity impact load," *Proc. Inst. Civ. Eng. Struct. Build.*, vol. 173, no. 8, pp. 549–567, 2020, doi: 10.1680/jstbu.18.00041.
- [18] M. A. Knott and O. D. Larsen, "Guide Specification and Commentary for Vessel Collision Design of Highway Bridges, Volume I: Final Report," 1990.
- [19] N. C. Street and N. W. Suite, *American Association of State Highway and Transportation Officials Washington , DC 20001 © 2012 by the American Association of State Highway and Transportation Officials . All rights reserved . Duplication is a violation of applicable law . Pub Code : LRF. 2012.*
- [20] E. C. for S. (CEN), "Eurocode 1 - Actions on structures - Part 1-7: General actions - Accidental actions," 2011.
- [21] J. Wang, D. Ph. L. Bu, and C. Cao, "Code Formulas for Ship-Impact Design of Bridges," no. August, pp. 599–606, 2012, doi: 10.1061/(ASCE)BE.1943-5592.0000289.
- [22] B. Liu, W. Fan, W. Guo, B. Chen, and R. Liu, "Experimental investigation and improved FE modeling of axially-loaded circular RC columns under lateral impact loading," *Eng. Struct.*, vol. 152, pp. 619–642, 2017, doi: 10.1016/j.engstruct.2017.09.009.
- [23] X. Zhou, M. Zhou, D. Luo, B. Wu, and L. Liu, "Study on the nonlinear response and shear behavior of RC columns under lateral impact," *Structures*, vol. 34, no. December 2021, pp. 3834–3850, 2021, doi: 10.1016/j.istruc.2021.09.094.
- [24] Z. Huang *et al.*, "Experimental and numerical study of the performance of geopolymer concrete columns reinforced with BFRP bars subjected to lateral impact loading," *Constr. Build. Mater.*, vol. 357, no. October, 2022, doi: 10.1016/j.conbuildmat.2022.129362.
- [25] X. Zhang, H. Hao, and C. Li, "The effect of concrete shear key on the performance of segmental columns subjected to impact loading," 2017, doi: 10.1177/1369433216650210.
- [26] R. W. Li, D. Y. Zhou, and H. Wu, "Journal Pre-proofs," 2019, doi: 10.1016/j.engfailanal.2019.104319.
- [27] T. Yilmaz, N. Kiraç, and Ö. Anil, "Experimental investigation of axially loaded reinforced concrete square column subjected to lateral low-velocity impact loading," *Struct. Concr.*, vol. 20, no. 4, pp. 1358–1378, 2019, doi: 10.1002/suco.201800276.
- [28] C. Demartino, J. G. Wu, and Y. Xiao, "Response of shear-deficient reinforced circular RC columns under lateral impact loading," *Int. J. Impact Eng.*, vol. 109, pp. 196–213, 2017, doi: 10.1016/j.ijimpeng.2017.06.011.
- [29] S. Xiang *et al.*, "Experimental study on the dynamic behavior of T-shaped steel reinforced concrete columns under impact loading," 2020.
- [30] X. Wang, A. Zheng, and Y. Hou, "Study on Impact Resistance of All-Lightweight Concrete Columns Based on Reinforcement Ratio and Stirrup Ratio," pp. 1–21, 2025.
- [31] J.-M. Sun, W.-J. Yi, H. Chen, F. Peng, Y. Zhou, and W.-X. Zhang, "Dynamic Responses of RC Columns under Axial Load and Lateral Impact," *J. Struct. Eng.*, vol. 149, no. 1, 2023, doi: 10.1061/jsendh/steng-11612.
- [32] L. Chen, Y. Xiao, and S. El-Tawil, "Impact Tests of Model RC Columns by an Equivalent Truck Frame," *J. Struct. Eng.*, vol. 142, no. 5, pp. 1–12, 2016, doi: 10.1061/(asce)st.1943-541x.0001449.
- [33] J. Wei, J. Li, and C. Wu, "An experimental and numerical study of reinforced conventional concrete and ultra-high performance concrete columns under lateral impact loads," *Eng. Struct.*, vol. 201, no. July, p. 109822, 2019, doi: 10.1016/j.engstruct.2019.109822.
- [34] T. Pham, W. Chen, and H. Hao, "Review on Impact Response of Reinforced Concrete Beams : Contemporary Review on Impact Response of Reinforced Concrete Beams : Contemporary Understanding and Unsolved Problems," no. February, 2021, doi: 10.1177/1369433221997716.
- [35] M. Kwon and E. Spacone, "Three-dimensional finite element analyses of reinforced concrete columns," vol. 80, pp. 199–212, 2002.
- [36] M. Yu, X. X. Zha, and Y. C. Wang, "Behaviour of different types of columns under vehicle impact," 2007.
- [37] Y. Sha and H. Hao, "Laboratory tests and numerical simulations of barge impact on circular reinforced concrete piers," *Eng. Struct.*, vol. 46, pp. 593–605, 2013, doi: 10.1016/j.engstruct.2012.09.002.
- [38] D. Zhou and R. Li, "Damage assessment of bridge piers subjected to vehicle collision," 2018, doi: 10.1177/1369433218772344.
- [39] H. M. I. Thilakarathna, D. P. Thambiratnam, M. Dhanasekar, and N. Perera, "Numerical simulation of axially loaded concrete columns under transverse impact and vulnerability assessment," vol. 37, pp. 1100–1112, 2010.
- [40] W. Tantrapongsaton and C. Hansapinyo, "Impact response of reinforced concrete columns with different axial load under low-velocity impact loading," *Key Eng. Mater.*, vol. 803 KEM, no. 2017, pp. 322–330, 2019, doi:

10.4028/www.scientific.net/KEM.803.322.

- [41] W. Fan, B. Liu, and G. R. Consolazio, "Residual Capacity of Axially Loaded Circular RC Columns after Lateral Low-Velocity Impact," *J. Struct. Eng.*, vol. 145, no. 6, pp. 1–16, 2019, doi: 10.1061/(asce)st.1943-541x.0002324.
- [42] B. Liu, W. Fan, X. Huang, X. Shao, and L. Kang, "A Simplified Method to Predict Damage of Axially-Loaded Circular RC Columns Under Lateral Impact Loading," *Int. J. Concr. Struct. Mater.*, vol. 14, no. 1, 2020, doi: 10.1186/s40069-020-00406-z.
- [43] K. M. A. Sohel, K. Al-Jabri, and A. H. S. Al Abri, "Behavior and design of reinforced concrete building columns subjected to low-velocity car impact," *Structures*, vol. 26, no. April, pp. 601–616, 2020, doi: 10.1016/j.istruc.2020.04.054.
- [44] W. Zhao and J. Qian, "Resistance mechanism and reliability analysis of reinforced concrete columns subjected to lateral impact," *Int. J. Impact Eng.*, vol. 136, no. October 2019, p. 103413, 2020, doi: 10.1016/j.ijimpeng.2019.103413.
- [45] X. Li, Y. Yin, T. Li, X. Zhu, and R. Wang, "Analytical Study on Reinforced Concrete Columns and Composite Columns under Lateral Impact," *Coatings*, vol. 13, no. 1, 2023, doi: 10.3390/coatings13010152.

### **Acknowledgments**

Not applicable.

## Appendix

**Table A1.** Data collected from steel RC columns subjected to lateral impact

Reference	year	column	velocity(m\s)	Axial force(kN) /ratio %	B or D (mm)	L(mm)	H (mm)	longitudinal reinforcement \ratio	stirrups spacing\ratio	peak impact force (KN)	Deflections (mm)	F <sub>y</sub> (MPA)	E <sub>s</sub> (GPA)
Chen et al. [32]	2016	CC1	13.9	N.F	333		2000	16Ø8	6.5@333	238.4	7.3	2394.879	180
		CC2	13.3	N.F	333		2000	16Ø8	6.5@333	308.9	38.8	3394.852	180
		CC3	10.4	N.F	333		2000	16Ø8	6.5@333	320	44	3394.824	180
Demartino et al.[28]	2017	CH1	4.5	N.F	330		1700	0.9	0.3	952	66.9	24278	204
		CH2	4.5	N.F	330		1700	0.9	0.09	993	79.5	24278	204
		CM1	3	N.F	330		1700	0.9	0.3	643	17.3	24278	204
		CM2	3	N.F	330		1700	0.9	0.09	645	17.9	24278	204
		FH1	4.5	N.F	330		1700	0.9	0.3	1060	75.4	24278	204

Reference	year	column	velocity(m/s)	Axial force(kN) /ratio %	B or D (mm)	L(mm)	H (mm)	longitudinal reinforcement \ratio	stirrups spacing\ratio	peak impact force (KN)	Deflections (mm)	F <sub>y</sub> (MPA)	E <sub>s</sub> (GPA)
		FH2	4.5	N.F	330		1700	0.9	0.09	1030	80.1	24278	204
		FM1	3	N.F	330		1700	0.9	0.3	719	27.1	24278	204
		FM2	3	N.F	330		1700	0.9	0.09	676	31.2	24278	204
		FL1	2.25	N.F	330		1700	0.9	0.3	502	10.5	24278	204
		FL2	2.25	N.F	330		1700	0.9	0.09	505	9.5	24278	204
Liu et al.[22]	2017	E1F1	4.85	0	200		2200	1.92%	1.30%	480.3	33.3	3418.10	200
		E1F2	4.85	200	200		2200	1.92%	1.30%	515.3	24.5	3418.10	200
		E1F3	4.85	400	200		2200	1.92%	1.30%	511.7	20.3	3418.10	200
		E1F3L6	4.85	400	200		2200	0.96%	0.72%	519	27.1	3418.10	200
		E2F1	6.86	0	200		2200	1.92%	1.30%	563.2	79.2	3418.10	200
		E2F2	6.86	200	200		2200	1.92%	1.30%	671.7	62.5	3418.10	200
		E2F3	6.86	400	200		2200	1.92%	1.30%	617.4	58.8	3418.10	200
		E2F3L6	6.86	400	200		2200	0.96%	0.72%	695.5		3418.10	200
Anil et al.[17]	2018	10-150c	4.29	N.F	100	100	1500	4Ø8	Ø4@150	9	4.94	14700	200

Reference	year	column	velocity(m/s)	Axial force(kN) /ratio %	B or D (mm)	L(mm)	H (mm)	longitudinal reinforcement \ratio	stirrups spacing\ratio	peak impact force (KN)	Deflections (mm)	F <sub>y</sub> (MPA)	E <sub>s</sub> (GPA)
		10-150c	4.29	N.F	100	100	1500	4Ø8	Ø4@150	10	7.1	14700	200
		20-150c	4.29	N.F	100	100	1500	4Ø8	Ø4@150	24	11.92	24700	200
		10-300	4.29	N.F	100	100	1500	4Ø8	Ø4@150	26	15.12	14700	200
		10-300c	4.29	N.F	100	100	1500	4Ø8	Ø4@300	23	13.2	14700	200
		20-300c	4.29	N.F	100	100	1500	4Ø8	Ø4@300	21	12.2	24700	200
		20-300	4.29	N.F	100	100	1500	4Ø8	Ø4@300	24	17.7	24700	200
		20-150	4.29	N.F	100	100	1500	4Ø8	Ø4@150	25	12.39	24700	200
Wei et al.[33]	2019	RC-S-h1.5	5.42	200	168	168	2000	4Ø12	Ø10@200	280	62	45000	200
		RC-S-h1.25	4.95	200	168	168	2000	4Ø12	Ø10@200			45000	200
		UHPC-S-h1.5	5.42	200	168	168	2000	6Ø12	Ø10@200	520	30	150036	200
		UHPC-S-h1.75	5.86	200	168	168	2000	4Ø12	Ø10@200	525	36	150036	200
		RC-C-h1	4.43	200	168	168	2000	6Ø12	Ø10@200			45000	200

Reference	year	column	velocity(m\s)	Axial force(kN) /ratio %	B or D (mm)	L(mm)	H (mm)	longitudinal reinforcement \ratio	stirrups spacing\ratio	peak impact force (KN)	Deflections (mm)	F <sub>y</sub> (MPA)	E <sub>s</sub> (GPA)
		UHPC-C-h1	4.43	200	168	168	2000	6Ø12	Ø10@200	320	24	1500 3 6	200
Yilmaz et al.[27]	2019	1	4.43	0	100	100	1500	4Ø10	Ø8@150	15.88	9.41	4490 5	208
		2	5.42	0	100	100	1500	4Ø10	Ø8@150	25.32	14.42	4490 5	208
		3	4.43	20	100	100	1500	4Ø10	Ø8@150	15.94	7.96	4490 5	208
		4	5.42	20	100	100	1500	4Ø10	Ø8@150	25.87	12.26	4490 5	208
		5	4.43	40	100	100	1500	4Ø10	Ø8@150	15.97	6.92	4490 5	208
		6	5.42	40	100	100	1500	4Ø10	Ø8@150	26.05	10.96	4490 5	208
		7	4.43	60	100	100	1500	4Ø10	Ø8@150	16.88	5.89	4490 5	208
		8	5.42	60	100	100	1500	4Ø10	Ø8@150	26.19	9.27	4490 5	208
		9	4.43	0	100	100	1500	4Ø10	Ø8@300	15.47	14.97	4490 5	208
		10	5.42	0	100	100	1500	4Ø10	Ø8@300	26.03	38.94	4490 5	208
		11	4.43	20	100	100	1500	4Ø10	Ø8@300	15.98	12.63	4490 5	208
		12	5.42	20	100	100	1500	4Ø10	Ø8@300	26.37	25.65	4490 5	208

Reference	year	column	velocity(m\s)	Axial force(kN) /ratio %	B or D (mm)	L(mm)	H (mm)	longitudinal reinforcement \ratio	stirrups spacing\ratio	peak impact force (KN)	Deflections (mm)	F <sub>y</sub> (MPA)	E <sub>s</sub> (GPA)
		13	4.43	40	100	100	1500	4Ø10	Ø8@300	16	10.7	44905	208
		14	5.42	40	100	100	1500	4Ø10	Ø8@300	26.13	21.54	44905	208
		15	4.43	60	100	100	1500	4Ø10	Ø8@300	16.01	9.3	44905	208
		16	5.42	60	100	100	1500	4Ø10	Ø8@300	26.01	18.63	44905	208
Ye et al.[15]	2020	LDL120-0.1-1.4	0.8	0.1	120	120	1150	1.40%	Ø8@70	50.42	77.25	6408.8039	200
		LDL150-0.1-1.4	0.8	0.1	150	150	1150	1.40%	Ø8@70	56.88	58.08	6424.6039	200
		LDL180-0.1-1.4	0.8	0.1	180	180	1150	1.40%	Ø8@70	71.9	27.64	6470.4039	200
		MDL120-0.1-1.4	0.8	0.1	120	120	1150	1.40%	Ø8@70	34.98	67.3	6408.8039	200

Reference	year	column	velocity(m\s)	Axial force(kN) /ratio %	B or D (mm)	L(mm)	H (mm)	longitudinal reinforcement \ratio	stirrups spacing\ratio	peak impact force (KN)	Deflections (mm)	F <sub>y</sub> (MPA)	E <sub>s</sub> (GPA)
		MDL150-0.1-1.4	0.8	0.1	150	150	1150	1.40%	Ø8@70	44.46	40.12	6424.6039	200
		MDL180-0.1-1.4	0.8	0.1	180	180	1150	1.40%	Ø8@70	36.03	20.1	6470.4039	200
		MDL150-0.1-2	0.8	0.1	150	150	1150	2.00%	Ø8@70	40.26	37.37	6470.4039	200
		MDL150-0.1-2.7	0.8	0.1	150	150	1150	2.70%	Ø8@70	35.38	34.1	6465.3039	200
		MDL150-0-1.4	0.8	0	150	150	1150	1.40%	Ø8@70	28.55	48.03	6424.6039	200
		MDL150-0.2-1.4	0.8	0.2	150	150	1150	1.40%	Ø8@70	36.3	28.61	6424.6039	200

Reference	year	column	velocity(m\s)	Axial force(kN) /ratio %	B or D (mm)	L(mm)	H (mm)	longitudinal reinforcement \ratio	stirrups spacing\ratio	peak impact force (KN)	Deflections (mm)	F <sub>y</sub> (MPa)	E <sub>s</sub> (GPa)
												390	
		SDL120-0.1-1.4	0.8	0.1	120	120	1150	1.40%	Ø8@70	37.14	54.37	6408.8	200
		SDL150-0.1-1.4	0.8	0.1	150	150	1150	1.40%	Ø8@70	63.64	43.16	6424.6	200
		SDL180-0.1-1.4	0.8	0.1	180	180	1150	1.40%	Ø8@70	30.13	15.84	6470.4	200
		SDL120-0-1.4	0.8	0	120	120	1150	1.40%	Ø8@70	30.73	69.93	6408.8	200
Zhou et al. [23]	2021	Z1-150-0.2	4.5	0.2	340		2100	2.70%	150	2014	18.95	4400	205
		Z2-100-0.2	4.5	0.2	340		2100	2.70%	100	1908	20.35	4400	205
		Z3-50-0.2	4.5	0.3	340		2100	2.70%	50	1821	22.87	4400	205

Reference	year	column	velocity(m/s)	Axial force(kN) /ratio %	B or D (mm)	L(mm)	H (mm)	longitudinal reinforcement \ratio	stirrups spacing\ratio	peak impact force (KN)	Deflections (mm)	F <sub>y</sub> (MPA)	E <sub>s</sub> (GPA)
		Z4-50-0.3	4.5	0.4	340		2100	2.70%	50	2057	18.04	4400 2	205
		Z5-50-0.4	4.5		340		2100	2.70%	50	2248	16.56	4400 2	205
Luo et al. [13]	2023	C_1	2.4-6.3	0	140	140	600	4Ø8	Ø6@50	NF	NF	3 0	200
		C_2	2.4-6.3	0	140	140	800	4Ø8	Ø6@50	NF	NF	3 0	200
		C_3	2.4-6.3	0-0.8	200	200	800	4Ø8	Ø6@50	NF	NF	3 0	200
Sun et al.[31]	2023	C-0-H	4.58	0	200	200	2200	2.54%	0.71%	344.7	113.2	3482 5 8	200
		C-6-H	4.58	296	200	200	2200	2.54%	0.71%	495.7	109.7	3482 5	200
		C-12-H	4.58	597	200	200	2200	2.54%	0.71%	709.1	152.5	3482 7 9	200
		C-3-M	3.58	141	200	200	2200	2.54%	0.71%	426.4	65.2	3482 7 3	200
		C-6-M	3.58	294	200	200	2200	2.54%	0.71%	459.4	68.6	3482 6 4	200

Reference	year	column	velocity(m\s)	Axial force(kN) /ratio %	B or D (mm)	L(mm)	H (mm)	longitudinal reinforcement \ratio	stirrups spacing\ratio	peak impact force (KN)	Deflections (mm)	F <sub>y</sub> (MPA)	E <sub>s</sub> (GPA)
		C-6-L	2.58	291	200	200	2200	2.54%	0.71%	282.6	37.7	3482.6	200

Where, B: refers to the section width, L: refers to the section depth, D: refers to the section diameter, H: refers to the column height, f<sub>c</sub>: refers to the compressive strength of concrete, f<sub>y</sub>: refers to the yield strength of steel, E<sub>s</sub>: modulus of elasticity for steel

**Table A2.** Finite Element studies presented for columns subjected to lateral impact load

Reference	Year	Investigated parameters	Findings
Thilakarathna et al. [39]	2010	A nonlinear finite element model was developed in LS-DYNA and validated using experimental results, incorporating the effects of strain rate and concrete confinement	Columns fail mostly in shear or shear-flexural modes close to the supports, and the impact behavior is similar to quasi-static stress.
Gholipour et al. [14]	2018	Effect of Axial load	The greatest value of the impact force and the flexural moment each dramatically rise at the mid-span column as the axial load ratio rises with strong relationships. The plastic hinge's position relative to the column mid-span decreases as the axial load ratio rises.
		Effect of impact elevation	As the impact height decreased, the column's failure mode shifted from global-flexure to shear-flexural or global shear. which consistent with experimental study above
Do et al.[11]	2018	The effects of the dynamic impact loading on the axial force, the bending moment, the shear force, and the failure modes of the bridge column have been examined.	(1) Although it hasn't been discussed in the literature, the engine's mass has a significant impact on the PIF, the moment, the shear force, and ultimately the column damage. The vehicle's engine mass and impact velocity can be used to anticipate the peak impact force on a bridge column, and momentum-impulse conservation can be used to estimate the collision's impulse.

Reference	Year	Investigated parameters	Findings
Tantrapongsaton & Hansapinyo [40]	2019	Effect of Axial Load	The peak impact force rises as column axial force increases, but the impact time decreases. As well as, when the column's axial force increased, there is a drop occur in the peak mid-span deflection. Furthermore axial load has a good influence on preventing cracks.
		Effect of Shear Stirrup Spacing.	Increase shear spacing has a good effect on increasing column impact force. It found that the member's shear capacity will regulate the deflection if it has a comparable bending capacity.
		Effect of Longitudinal Steel Bar Size/Stirrup Size.	It can be inferred that a reduced impact force is the result of a lowered column's bending ability. It may be inferred that the bending capacity above the shear capacity was mostly responsible for the RC column's deflection under impact force.
Fan et al. [41]	2019	Effect of Axial Load Ratio	From 0.1 to 0.3, the residual strength rose as the axial load ratio increased. The test findings showed that the applied axial load tended to enhance impact resistance by strengthening the concrete's confinement effect when impact-induced damage was minimal.
		Effect of Longitudinal Reinforcement Ratio	The longitudinal reinforcement ratio had no considerable effect on the residual strength of the damaged column when the transverse reinforcement ratio was quite high. This was explained by the fact that the axial capacity of a column with a relatively high transverse reinforcement ratio primarily relies on the area of confined concrete, as opposed to the amount of longitudinal reinforcement available.
		Effect of transverse reinforcement ratio	Compared to columns with low reinforcement ratios, those with high transverse reinforcement ratios showed greater residual strengths.

Reference	Year	Investigated parameters	Findings
Wei et al.[33]	2020	Column width	It is evident that columns having a greater cross-section are more resistant to impact because An excessive section modulus and mass.
		Column depth	Both the mass and velocity asymptotes of M-V diagrams rise as column depth increases. Column depth has more effect than width. significant impact on the resistance to impact.
		Column height	It may be observed by comparing the mass and velocity asymptotes that both asymptotes somewhat drop as column height increases. The findings show that narrow columns are more prone to flexural failure brought on by impacts.
		Concrete strength	It is evident that the mass and velocity asymptotes are positively impacted by the strength of the concrete.
		Longitudinal reinforcement	The mass and velocity values of the mass-velocity curve are able to raise by increasing the longitudinal reinforcement ratio in compression. The column's bending strength will be significantly increased by the longitudinal reinforcement ratio, which explains this. The advantages of using UHPC in protective structural design are further highlighted by the fact that the columns maintain a respectable impact resistance despite less longitudinal reinforcement.
		Axial loads	The results suggest that the rising axial loads could raise mass and velocity asymptotes.
Liu et al. [42]	2020	Effect of Axial Load	The column's damage decreased as axial load ratios increased (from 7 to 28%) under the same energy inputs.

Reference	Year	Investigated parameters	Findings
		effect of reinforcement ratio	Increasing reinforcement ratios can greatly improve the RC column's impact-resistant performance with the same axial stresses, because it increased the RC column's resistance to bending.
Sohel et al.[43]	2020	the effect of a car impact on an axially loaded building column is evaluated	<ol style="list-style-type: none"> <li>1. A automobile hit at a low velocity (<math>\leq 60</math> km/h) can cause an RC column with a smaller dimension (<math>\leq 300 \times 300</math> mm) to fail in shear.</li> <li>2. The impact event is significantly influenced by the column's axial load level. At a lower axial force ratio, the column undergoes greater lateral displacement. Compared to other columns bearing axial force, the column has the most lateral displacement with zero axial force. When the axial load level is less than 40% of the column's design capacity, the impact resistance drops.</li> </ol>
Zhao and Qian [44]	2020	impact velocity	The probability of shear failure increases significantly with impact velocity when it exceeds 5 m/s.
		projectile mass	The impact velocity has a greater impact on the structural reliability than the impact mass under the same impulse, it can be concluded.
		compressive strength	It has been noted that the column made of low-strength concrete is susceptible to lateral impact loads. In contrast to other factors, the likelihood of shear failure of the column is highly susceptible to the strength of the concrete.
		section width	Increasing the section area, particularly the section height, can significantly increase the dependability of RC columns under impact loads.
Luo et al.[13]	2023	effect of impact energy	The damage area greatly increased as the impact speed increased. Impact impulse and peak contact interface force increased in line with impact mass and velocity.

Reference	Year	Investigated parameters	Findings
		effect of reinforcement ratio	As the longitudinal reinforcement radius increased, localized contact stiffness and peak contact interface force also altered. The peak horizontal displacement and the residual column top displacement either decreased as the longitudinal reinforcement ratio.
		effect of stirrup	The maximum displacement and residual deformation of the RC columns decreased as the stirrup rose. Increasing the stirrup reinforcement ratio could improve the lateral impact resistance.
		effect of strength grade	The enhancement in concrete strength grade under the test conditions limited an enhancement in the model column's lateral impact resistance from the perspectives of total impact and local damage.
		effect of slenderness ratio	The ultimate contact interface force rose in tandem with column height.
		Effect of Axial Compression Ratio	As the rate of axial compression raised, the peak contact interface force rose under the same impact energy. Additionally, when the impact velocity rose, so did the contact holding duration and peak contact interface force at the equivalent axial pressure ratio.
Li et al.[45]	2023	compressive strength	The peak impact force rises as concrete's compressive strength does.
		diameter-thickness ratio	There is a negative correlation between the peak impact force and the diameter–thickness ratio of the inner and outer steel tubes.
		impact velocity	Impact velocity varies in the ascending region but has most impact in the decreasing region.

Reference	Year	Investigated parameters	Findings
		impact mass	The Impact mass and yield strength of the inner and outer steel tubes have a significant impact on peak deflection but minimal effect on impact peak force.